Deposition Temperature Dependency of Characteristics of PMnN-PZT Epitaxial Thin Film on Si Prepared by Sputter Deposition with Fast Cooling

Tohoku Univ., °Zhen Zhou, Shinya Yoshida, Shuji Tanaka
E-mail: zhouzhen@mems.mech.tohoku.ac.jp

As a high performance piezoelectric thin film for MEMS (Micro Electro Mechanical Systems) sensors, a highly *c*-axis oriented $Pb(Mn_{1/3}, Nb_{2/3})O_3$-$Pb(Zr, Ti)O_3$ (PMnN-PZT) epitaxial thin film has been formed on a Si substrate by sputter deposition with fast cooling [1]. This process forcibly suppresses *a*-domain generation contributing to tensile stress relaxation during the cooling process. In other words, a large tensile stress remains in the *c*-axis oriented thin film. Such a large tensile stress has a risk to lead crack generation after deposition or during actuation.

The tensile stress reduction will be achieved by lowering the deposition temperature. However, nobody has investigated the dependency of the characteristics of the PMnN-PZT epitaxial thin film on the deposition temperature in detail. On the other hand, Wasa *et al.* recently published an interesting report that the stress of a fast-cooled PMnN-PZT epitaxial thin films on a $SrRuO_3$(SRO)/Pt/MgO substrate was released by atomic defects at the interface between PMnN-PZT and SRO [2]. It is interesting whether such a stress release mechanism also works for the film on a Si substrate.

In this study, PMnN-PZT epitaxial thin films were deposited by sputtering on SRO/$La_{0.5}Sr_{0.5}CoO_3$ /CeO_2/yttria-stabilized zirconia/Si substrates at various temperatures. The films were investigated in terms of residual tensile stress, lattice parameters, ferroelectric, dielectric and piezoelectric properties.

Figure 1 shows θ-2θ X-Ray Diffraction (XRD) spectra of the PMnN-PZT thin films deposited at various deposition temperature. As shown in this figure, the epitaxy arose at higher than 500°C. The *c*-axis orientation degree of each epitaxial thin film was estimated to be about 90%. Figure 2 compares the lattice parameters of the samples prepared at different temperatures. The tetragonality of the *c*-domain as the major domain decreased as the deposition temperature decreased.

Considering thermal stress, the in-plane tensile stress of the film deposited at higher temperature should be larger. A large stress should decrease the tetragonality of the *c*-domain due to *a*-domain generation. However, what was observed in Fig. 2 is the contrary. On the other hand, the tetragonality of the *a*-domain significantly decreased with decrease in deposition temperature, which can be simply explained by thermal stress. Compared to the *a*-domain, the *c*-domain crystalline structure looked more rigid and insensitive to the stress. This mechanism has not been clarified, but strong binding of the *c*-domain and SRO crystalline lattice with a smaller lattice parameter may be one of factors. In addition, the stress of the *c*-domain might be released partially due to generation of the atomic defects at the interface. This experimental result indicates that the higher deposition temperature leads to higher tetragonality of both *c*-domain and *a*-domain.

The residual stress was qualitatively compared among the thin films with various thicknesses by observing crack generation. As a result, the crack was often generated in the 2-μm thick film deposited at 600°C and 550°C, while no crack was generated in the same thickness of films prepared at 500°C. Thus, we conclude that the residual tensile stress was not dramatically released unlike the case for MgO substrate, and high temperature deposition led to higher tensile stress even if the atomic defects was generated.

We will report on the ferroelectric, dielectric, and piezoelectric properties of each sample at the meeting.

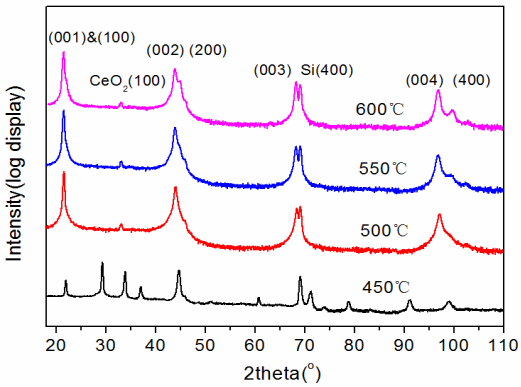

Fig. 1. θ-2θ XRD spectra of the PMnN-PZT thin films deposited at various deposition temperatures.

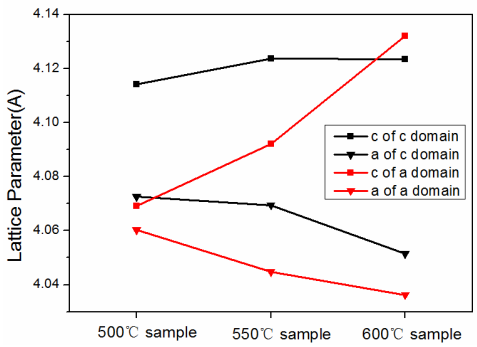

Fig. 2. Lattice parameters of *a* and *c* domain of PMnN-PZT thin films deposited at different temperature.

[1] Yoshida, S., et. al. (2016). Sensors and Actuators A: Physical, 239, 201–208.
[2] Wasa, K., et. al. (2015). Journal of Applied Physics, 117(12), 124106.